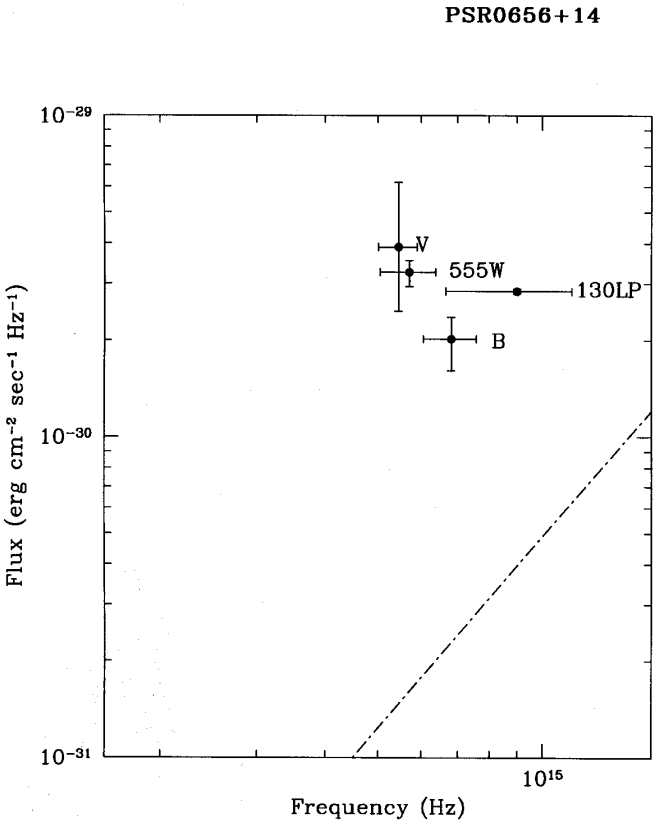

Figure 2: Colours of PSR 0656 +14 compared with the Rayleigh-Jeans extrapolation of the soft X-ray spectrum ($T \sim 8 \cdot 10^5$ K) as observed by the ROSAT/PSPC (Finley et al., 1992). The optical/UV fluxes have been corrected for the interstellar extinction using the N_H best fitting the ROSAT data ($N_H \sim 10^{20}$ cm^{-2}) and correspond to the original detection in the V band (Caraveo et al, 1994a), to the HST observation in the 555W filter (see text), to the FOC observation of Pavlov et al. (1996) in the 130LP filter and to the B photometry of Shrearer et al. (1996). The points are at least 2 magnitudes above the expectations.

the position of the reference stars does not change noticeably, a trend is recognisable for the proposed candidate.

Unfortunately, the factor of ten difference in the pixel size between the ESO images and the PC one translates into a large error of the object relative position as computed in the 1989 and 1991 frames, thus making it difficult to reliably compute its displacement. After fitting the object positions at different epochs, we obtain a value $\mu = 0.107 \pm 0.044$ arcsec/yr with a corresponding position angle of $112° \pm 9°$ to be compared with the radio values obtained by Thompson and Cordova (1994). Although not statistically compelling, a hint of proper motion is certainly present in our data.

4. Conclusions

Proper motion appears to be a powerful tool to secure optical identifications of candidate counterparts of INSs, as successfully shown for Geminga (Bignami et al., 1993). Its application is straightforward, just relying on deep, high-quality imaging.

Following this strategy, we have used our ESO 3.6-m/NTT images plus a more recent HST/PC one, to measure the proper motion of the candidate counterpart of PSR 0656 +14. Although promising, this case is not settled yet. The significant uncertainty makes the present result tantalising but certainly far from being conclusive. Of course, new high-resolution observations, could easily say the final word. Again, these could be obtained with the PC or, from the ground, using the VLT.

A firm optical identification of PSR 0656 +14 would be important to establish its emission mechanism in the optical domain and, thus, to complete the multiwavelength phenomenology of this source. The multicolour data presently available (Pavlov et al., 1996; Mignani et al., 1997a), are not easily compatible with the Rayleigh-Jeans extrapolation of the soft X-ray Planckian, even considering the spectral distortion induced by an atmosphere around the neutron star (Meyer et al., 1994). New, as yet unpublished FOC observations in the B/UV (Pavlov, 1996, private communication) seem to confirm this finding which appears to be further substantiated by the possible detection of optical pulsations (Shrearer et al., 1996), accounting for almost 100% of the flux in the B band (B $\sim$ 25.9) More colours of the counterpart are needed to understand the optical behaviour of the source. Now that the FOC has explored the B side of the spectrum, it is mandatory to concentrate on the Red part seeking for an R or I detection. NTT time has been granted for this project and the observations are currently underway.

Acknowledgements. R. Mignani is glad to thank J. Trümper and M.-H. Ulrich for the critical reading of the paper.

References

Becker, W., 1996, in Proc. of Würzburg Conference Roentgenstrahlung from the Universe, MPE Report **263**,103.
Bignami, G.F. et al., 1987 *Ap.J.* **319**, 358.
Bignami, G.F., Caraveo P.A. and Mereghetti, S., 1993 *Nature* **361**, 704.
Caraveo, P.A, 1993 *Ap.J.* **415**, L111.
Caraveo, P.A., Bignami, G.F. and Mereghetti, S., 1994a *Ap.J.* Lett. **422**, L87.
Caraveo, P.A., Bignami, G.F. and Mereghetti, S., 1994b *Ap.J.* Lett. **423**, L125.
Caraveo, P.A., Bignami, G.F, Mignani, R. and Taff, L., 1996, *Ap.J.* Lett. **461**, L91.
Caraveo, P.A., 1996, *Adv. Sp. Res.* in press.
Finley, J.P., Ögelman, H. and Kiziloglu, U, 1992 *Ap.J.* **394**, L21.
Lyne A. and Lorimer D., *Nature* **369**, 127.
Meyer, R.D. et al, 1994 *Ap.J.* **433**, 265.
Mignani, R., Caraveo, P.A. and Bignami, G.F., 1997a, *Adv. Sp. Res.* in press.
Mignani, R., Caraveo, P.A. and Bignami, G.F., 1997b, *Ap.J.* Lett, **474**, L51.
Pavlov, G.G., Strigfellow, G.S. & Cordova, F.A., 1996, *Ap.J.* **467**, 370 .
Ramanamurthy P.V. et al 1996 *Ap.J.* **458**, 755.
Shrearer A. et al 1996 IAUC 6502.
Thompson, R.J. and Cordova, F.A., 1994 *Ap.J.* **421**, L13.

rmignani@rosat.mpe-garching.mpg.de

On the Nature of the High-Redshift Universe

S. SAVAGLIO, ESO

One of the most debated arguments of recent astronomy is the understanding of the physical conditions of the Intergalactic Medium (IGM) at high redshift since it represents a unique probe of the young Universe. The state of the diffuse matter, the formation and distribution of the first collapsed objects, their nature and evolution with redshift are all open questions strongly related to the origin of the Universe. The most distant and powerful sources, the quasars, offer the opportunity to explore this side of the Universe.

The optical part of high redshift quasar spectra ($z > 2$) manifests the presence of a high number of Lyα absorption lines due to neutral hydrogen. For very

distant objects, suitable observations are guaranteed only by 4-m-class or larger telescopes. In this paper, new results on the $z \sim 4$ Universe obtained with EMMI observations (the high-resolution echelle spectrograph mounted at the ESO New Technology Telescope) of the high-redshift quasar Q0000-26 will be presented. These data are part of a sample of high-redshift QSO observations obtained during the ESO Key Programme 2-013-49K devoted to study the Intergalactic Medium at high redshift (P.I. S. D'Odorico).

The light emitted by Q0000-26 (at a redshift of $z = 4.12$) scans the Universe starting at an epoch when it was only 10% of its present age (for a flat Universe with $q_0 = 0.5$). Since it is one of the most distant and intrinsically brightest objects, it has been observed several times in the past. Recently, new observations at high resolution and signal-to-noise ratio have been presented almost simultaneously by two different groups of astronomers: by Lu et al. (1996) using the 10-m Keck Telescope and by Savaglio et al. (1996) with the ESO 3.5-m NTT. In Figure 1, an interesting comparison between the two spectra is shown. In that spectral range, the Keck spectrum has a resolution of FWHM = 6.6 km s^{-1} for a total exposure time of 12,000 seconds. The NTT observations in the same spectral range have a resolution of FWHM = 13 km s^{-1} and a total exposure time of 27,600 seconds. One may notice that all the information contained in the Keck observations can be found in the NTT ones, even if the resolution is considerably better in the former. This means that higher resolution does not help in overcoming an intrinsic limitation of the high-redshift QSO observations due the confusion of the absorption lines. The signal-to-noise ratio is similar in the two spectra, which is what one would expect comparing the exposure times and the different collecting areas. Remarkable differences in the interpretations of the data are due to the line-fitting procedure used.

The majority of the very numerous lines seen in QSO spectra has HI column densities below $N_{HI} \sim 10^{15}$ cm^{-2}. Higher HI column density systems ($N_{HI} \gtrsim 10^{16}$ cm^{-2}) frequently show associated metal lines which probably have origin in protogalactic halo or disk clouds. In the past, astronomers have raised a still unresolved question on the nature of the low HI column density ($N_{HI} \lesssim 10^{15}$ cm^{-2}) clouds, commonly referred to as Lyα forest. In particular, they have been thought for a long time to be intergalactic gas clouds of primordial chemical composition not associated with galaxies. Only the recent performances of optical telescopes allowed to see in more detail the QSO spectra at the expected positions of the metal lines associated with the Lyα lines and to give new constraints on the chemical composition and evolutionary state of those clouds. The NTT observations revealed the presence of C IV and Si IV in three optically thin HI clouds in the redshift range $3.5 < z < 3.8$ (Savaglio et al., 1996). The age of these clouds, assum-

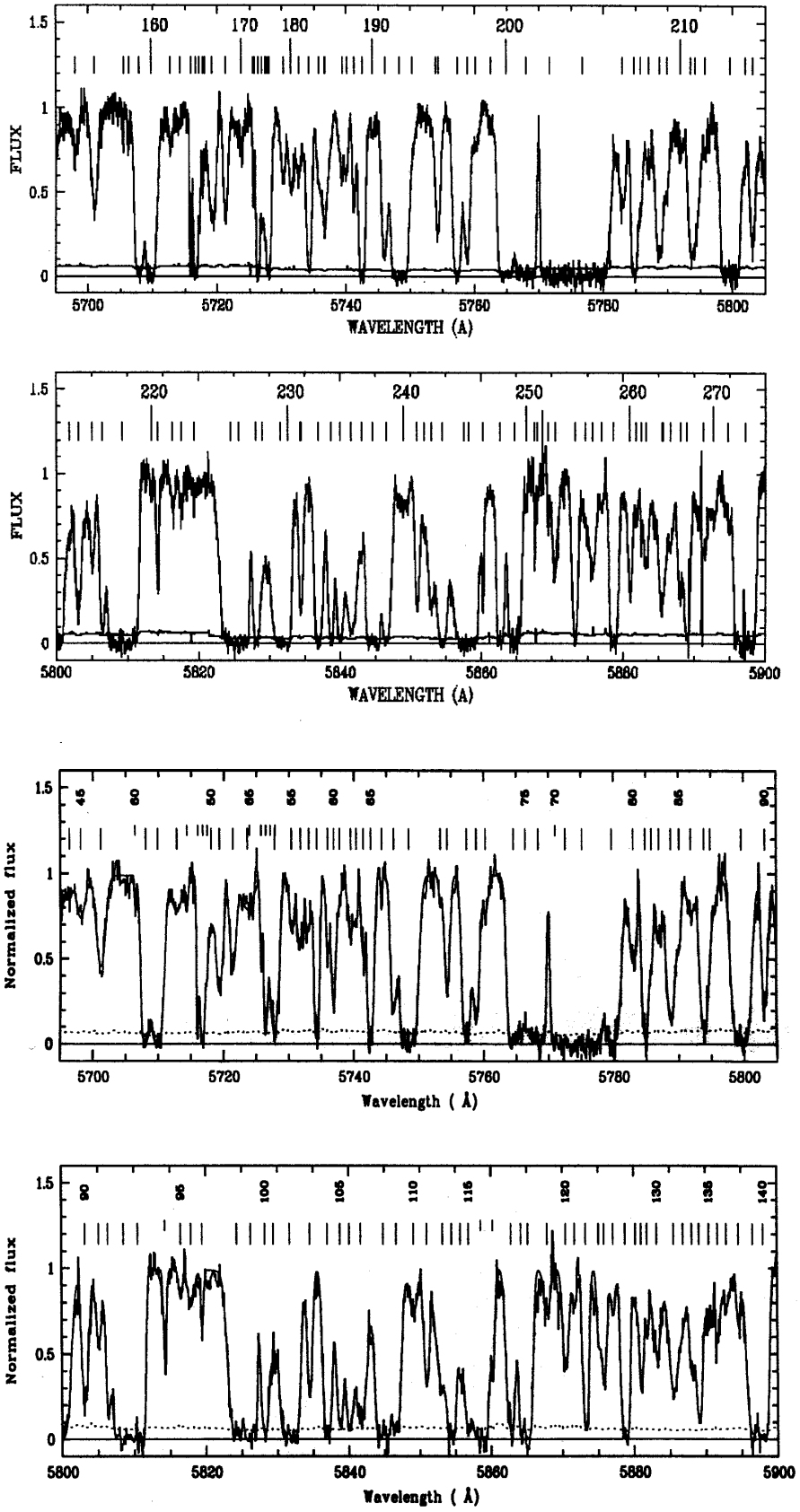

Figure 1: Spectrum of the high redshift quasar Q0000-26 (z = 4.12). The two upper panels have been obtained with the 10-m Keck telescope (Lu et al., 1996) at a resolution of FWHM = 6.6 km s^{-1} and an exposure time of 12,000 seconds. The two lower panels are NTT data (Savaglio et al., 1996) in the same spectral range at a resolution of FWHM = 13 km s^{-1} and an exposure time of 27,600 seconds.

ing that they are connected to galaxy formation and the redshift of galaxy formation is not beyond $z_f = 10$, is lower than 1.4 Gyr (for $H_0 = 75$ km s^{-1} Mpc^{-1} and $q_0 = 0.1$) or 0.9 Gyr (for $H_0 = 50$ km s^{-1} Mpc^{-1} and $q_0 = 0.5$).

To investigate the physical state of these systems, namely their ionisation state, density and size, it is possible to model the observed parameters of the clouds. Optically thin systems at high redshift with metal absorption lines are particularly interesting by themselves, not only because they are related to the early phases of galaxy evolution, but also because their ionisation state is probably dominated by the UV background flux, thus providing indirect information on the IGM.

The UV background (UVB) radiation field at high redshift is the result of the integrated light of the collapsed objects at early epoch once the absorption due to both diffuse IGM and discrete clouds is taken into account. Its shape, intensity and redshift dependence ($J_\nu(z)$) is a subject of controversy both from the theoretical and observational point of view. Direct estimates at the Lyman limit wavelength $\lambda_{LL} = 912$ Å as a function of redshift ($J_{912}(z)$) can be given by comparing the ionisation state of the clouds close to the quasar with those far from the quasar and presumably ionised by the UVB. Modelling of $J_\nu(z)$ has been mostly done considering the quasar integrated light only (Haardt & Madau, 1996). The effects of the presence of a population of young galaxies have been discussed by Miralda-Escude & Ostriker (1990). The soft spectrum of young galaxies would cause an increase of the jump of the UVB at the two edges of the Lyman limit wavelengths for H I and He II, namely $S_L = J_{912}/J_{228}$. The same effect would be obtained if an absorption of He II in the diffuse IGM were considered. The amount of He II in the IGM has not been firmly established yet and it will necessitate further efforts with HST observations for more significant estimates.

Figure 2 shows the details of possible UVB spectra. For three different values of log $S_L = 2$, 2.9, 3.5, three different spectral shapes in the range $1 \leq \nu/\nu_{LL} \leq 4$ (912 Å $\geq \lambda \geq$ 228 Å) can be considered. Also indicated as dotted vertical lines are the ionisation potential of the most interesting species. It is clear that the abundances of these species depends not only on S_L but also on the shape of J_ν for $4 \leq \nu/\nu_{LL} \leq 1$.

Given the shape and intensity of the UVB, it is possible to explore the parameter space using the observed ion abundances. Figure 3 shows the results of photoionisation calculations using CLOUDY (Ferland, 1993) applied to one of the optically thin systems in Q0000-26 at $z = 3.8190$ observed with the NTT. The UVB spectra used as ionising sources are those indicated in Figure 2.

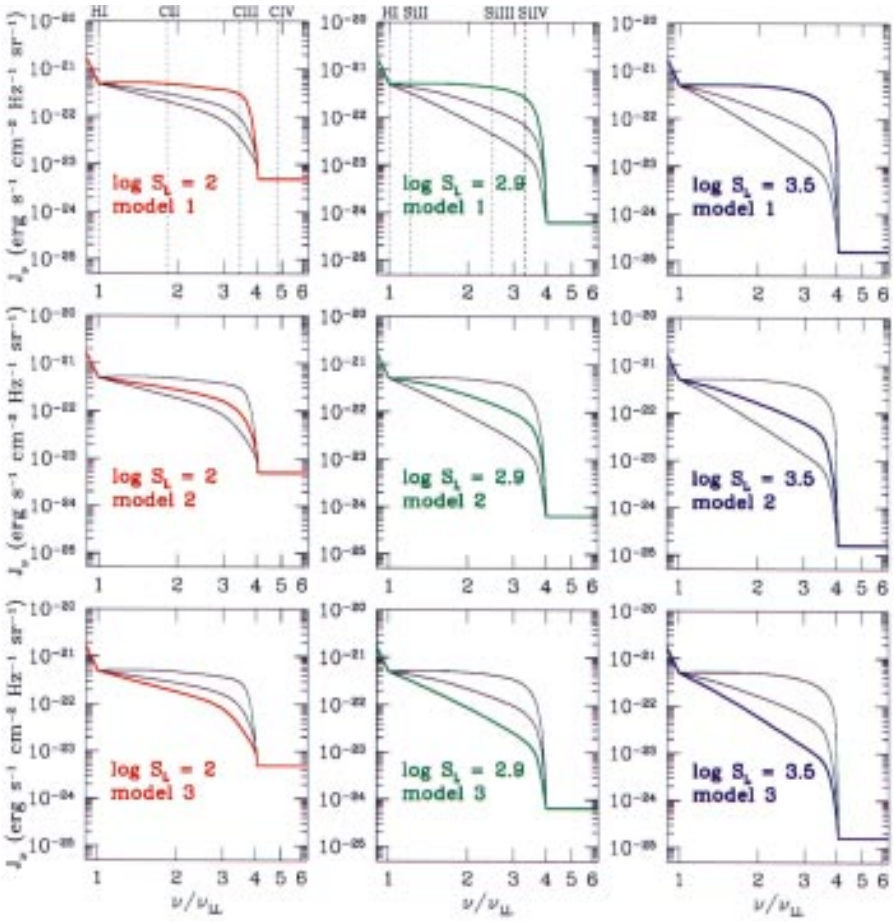

Figure 2: Models of the UV ionising background as a function of the frequency. The red, green and blue curves indicate the models with log $S_L = 2$, 2.9 and 3.5, respectively. For each value of S_L three different shapes of J_ν in the frequency interval $1 \leq \nu/\nu_{LL} \leq 4$ are shown. The vertical dotted lines indicate the values of ionisation potential for species of interest.

The values of silicon-to-carbon ratios are shown as a function of the carbon abundances [C/H] for different values of the gas density obtained forcing the code to reproduce the observed H I and C IV column densities.

In the study of the heavy element abundances of the Interstellar Medium (ISM) and stars, the abundance measurements are usually reported as a function of the iron-to-hydrogen ratio since the iron content is usually considered an age estimator (Timmes et al., 1995). The evolution of carbon in disk and halo stars follows that of iron. In fact, iron is mainly produced by type Ia Supernovae, while carbon is supposed to be mainly produced by intermediate-mass stars and these two processes have similar time scales. The silicon history is different being higher than in the sun for low metallicity, since the intermediate-mass α-chain elements are formed early by type II Supernova events. In QSO absorption lines, carbon is easier to detect than iron, therefore, normally, in absence of iron, carbon is considered for metallicity evaluations assuming that carbon abundance evolution follows that of iron. This is justified by models of chemical evolution, even though observations show a large spread with no particular trend (Timmes et al., 1995). Comparisons with the local ISM abundances are complicated by the fact that iron is strongly depleted into dust grains, both in warm and cold gas (–1.4 *dex* in the first and –2.2 *dex* in the second, Lauroesch et al., 1996) whereas carbon is much less hidden into dust grains, its depletion being around –0.3 *dex.* Therefore, considering the carbon abundance as metallicity indicator has the advantage that depletion in low-density gas is negligible, especially at high redshift when the dust formation is probably in an early phase. The red lines in Figure 3 represent the silicon over-abundance with respect to carbon as a function of metallicity as found by chemical evolution models.

Another interesting parameter which can be explored by photoionisation calculations is the physical size of the absorbing cloud. The regions with $R >$ 50 kpc and $R <$ 1 kpc are represented by the left and right shaded regions, respectively, in Figure 3. The green dot in each panel represents the result for a gas density of $n_H = 10^{-3.1}$ cm^{-3}. Dots towards lower metallicity represent gas densities decreasing by steps of 0.2 *dex,* and vice versa for dots towards higher metallicities.

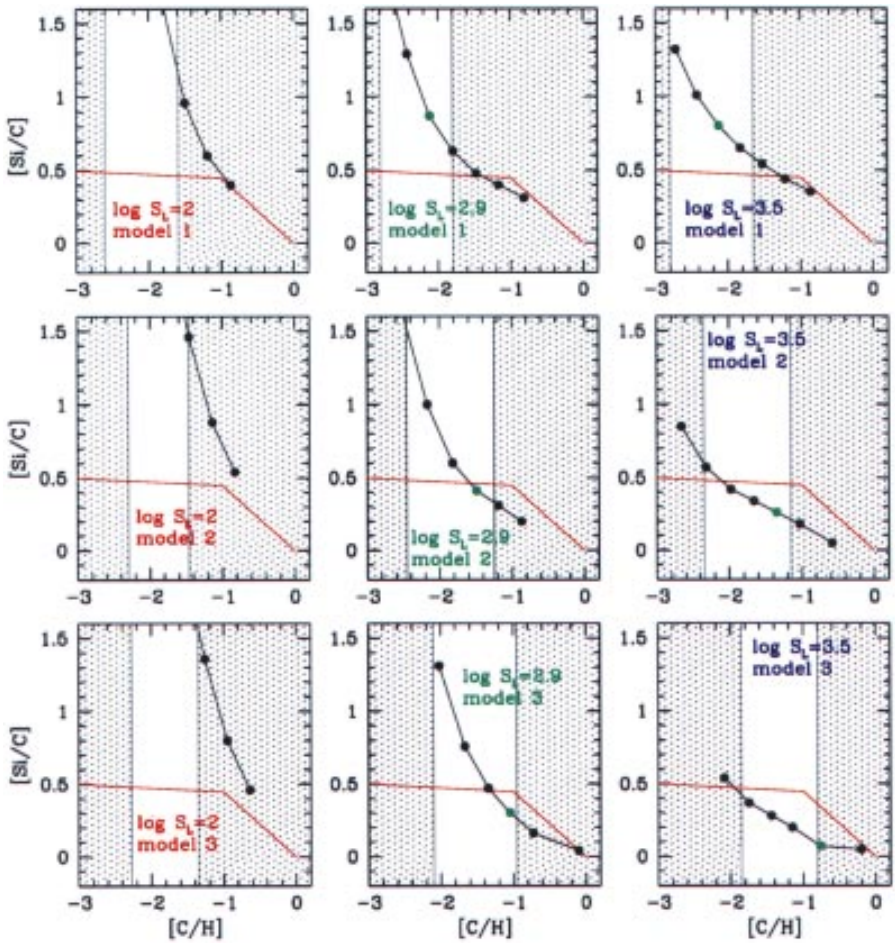

Figure 3: Silicon-to-carbon ratio as a function of the carbon-to-hydrogen ratio for the absorbing system at z = 3.8190 observed in Q0000-26 ([X/Y] = log(X/Y)$_\odot$ – log(X/Y)). Both values are compared to the solar values. The dots are results of CLOUDY calculations obtained varying the gas density n_H with a 0.2 dex step. The green dot indicates the result for log n_H = –3.1. Lower densities have higher [C/H] values, while higher densities have lower [C/H] values. The shaded areas indicate the regions where the cloud sizes become smaller than 1 kpc (right side) or larger than 50 kpc (left side). The results are shown for three different models of J_ν and three different S_L values.

The expected values of [Si/C] can be reproduced by the models with log S_L = 2 only assuming a cloud size by far smaller than 1 kpc and this would give a metallicity for this cloud larger than 1/10 of solar. Therefore, observations can be better explained only if log $S_L > 2$. The metallicity in log $S_L = 2.9$ models is in the range $-2.2 \lesssim$ [C/H] $\lesssim -1$, while the density spread is $-3.5 \lesssim \log n_H \lesssim -2.9$. A similar spread in metallicity is obtained for the log $S_L = 3.5$ models, whereas the upper limit to the density is log $n_H \lesssim -3.7$. Metallicities lower than 1/10 of solar found in this cloud, suggest ages lower than 1 Gyr. The size inferred by the calculations indicates that the cloud is smaller than typical clouds of the Lyα forest for which lower limits to the size have been found to be 70 kpc (for H_0 = 70 km s^{-1} Mpc^{-1}) at redshift $z \sim 2$ (Smette et al., 1995). The difference is also in the gas density which is always lower than the typical value of $n_H = 10^{-4}$ cm^{-3} found in the Lyα forest clouds. Thus we are still far from concluding that all the optically thin Lyα lines have the same intergalactic origin.

Metal systems optically thin to the HI ionising photons are an important probe of the shape of the UV background radiation. If this is the main ionising source, the quasar light contribution only absorbed by H I of the discrete Lyα clouds and Lyman limit systems (which implies log $S_l \sim 1.5$) cannot explain the observations. This means that either an additional source of ionisation is necessary, or intergalactic diffuse He II is responsible for the spectral shape of J_ν at wavelengths lower than 228 Å, or both. Further detailed analysis of $N_{\rm HI} \sim 10^{15}$ cm^{-2} absorption systems with metal lines will hopefully clarify this situation. Challenging results can be obtained by dedicated observations with 4-m-class telescopes and do not need to wait for the VLT to be operational.

References

Ferland G.J., 1993, University of Kentucky, Department of Physics and Astronomy Internal Report.

Haardt F., Madau P., 1996, *ApJ*, **461**, 20.

Lauroesch J.T., Truran J.W., Welty D.E., York D.G., 1996, *PASP*, **726**, 641.

Lu L., Sargent W.L.W., Womble D.S., Takada-Hidai M., 1996, *ApJ*, **472**, 509.

Miralda-Escude J., Ostriker J.P., 1990, *ApJ*, **350**, 1.

Savaglio S., Cristiani S., D'Odorico S., Fontana A., Giallongo E., 1996 *A&A*, *in press.*

Smette A., Robertson J.G., Shaver P.A., Reimers D., Wisotzki L., Köhler T., 1995, *A&AS*, **113**, 199.

Timmes F.X., Woosley S.E., Weaver T.A., 1995, *ApJS*, **98**, 617.

Sandra Savaglio, e-mail: ssavagli@eso.org

Optical Observations Provide a New Measure of the Vela Pulsar's Proper Motion

F.P. NASUTI[1], R. MIGNANI[2,1], P.A. CARAVEO[1] and G.F. BIGNAMI[1,3]

[1] *Istituto di Fisica Cosmica del CNR, Milano, Italy*
[2] *Max-Plack-Institut für Extraterrestrische Physik, Garching*
[3] *Dipartimento di Ingegneria Industriale, Università di Cassino, Italy*

1. Introduction

Isolated Neutron Stars (INSs) move in the sky with high (≥ 100 km s^{-1}) tangential velocities (Lyne & Lorimer, 1994). Indeed, proper motions have been measured for several INSs, mainly in the radio domain (Harrison et al., 1993). In addition, for two (possibly three) INSs proper motions have been measured in the optical domain through relative astrometry of their optical counterparts.